Artificial Life and Robotics (2018) 23:585–592
https://doi.org/10.1007/s10015-018-0492-4

ORIGINAL ARTICLE

Efficiency analysis of telescopic-legged bipedal robots

Yuji Harata[1] · Yotaro Kato[2] · Fumihiko Asano[3]

Received: 2 May 2018 / Accepted: 18 September 2018 / Published online: 1 October 2018

Abstract
This paper investigates the stability of underactuated bipedal walking incorporating telescopic-leg actuation. In human walking, knee joints of swing and support legs are bent and stretched. The telescopic legs mimic the motion of the center of mass of human legs via their telescopic motion during the stance phase. First, underactuated telescopic-legged biped robot models are introduced. Second, an output-following control law is applied to the linearized equation of motion of the robot, and the controlled robot's equation is then specified as a linear time-varying system. The error transition equation is developed to evaluate the stability during the stance phase. Numerical calculations are performed to show the influences of leg telescopic motion on the stability.

Keywords Bipedal locomotion · Stability · Time-varying system · Telescopic legs

1 Introduction

Many researchers have investigated limit cycle walking, such as passive dynamic walking [1–3]. In limit cycle bipedal walking, when a robot starts to walking from adequate initial conditions, robot's states converge to that of steady-state walking, and hence, the walks are inherently stable. However, many limit cycle-walking methods are not robust against disturbances. Therefore, robust controllers are needed for biped robots to avoid falling down. To do so, we should evaluate stability of generated walking and control the motion of a biped robot based on its stability. As the first step to the goal, we aim to establish the method that evaluates the stability of the steady walking in this paper.

In human walking, knee and elbow joints are often bent and stretched. These motions make the center of mass (COM) of legs and arms move up and down. Asano and Luo have mimicked these motion of a swing leg using a telescopic leg and proposed stable gait generation method [4]. Hanazawa et al. have focused on up and down motions of COM due to swing arms and achieved high-speed walking by controlling COM motion [5]. In the previous research, the influences of the up and down motions of COM on the walking speed and energy efficiency have been shown, but its stability has not been investigated.

To determine stability of limit cycle walking, some kinds of methods are proposed. Basin of attraction of passive dynamic walking is calculated [6], and gait sensitivity norm evaluates disturbance rejection ability [7]. Theoretical analyses also performed for the limit cycle walking [8]. Asano [9, 10] analytically derived the transition function of the state error from the linearized equation of motion of walkers.

This paper investigates the stability of underactuated bipedal walking incorporating telescopic-leg actuation using Asano's methods [9, 10]. First, underactuated telescopic-legged biped robot models are introduced and the linearized equation of motion is derived. Second, an output-following control law is applied to the linearized model, and the controlled robot's equation is then specified as a linear time-varying system. This causes the difficulty of derivation of the transition matrix for the state error. We then use a method for approximate calculation to obtain the transition matrix, which can evaluate the stability of the stance phase. Our approach has the advantage that the scalar transition function for the state error can be uniquely determined, although

This work was presented in part at the 2nd International Symposium on Swarm Behavior and Bio-Inspired Robotics, Kyoto, October 29–November 1, 2017.

✉ Yuji Harata
y-harata@aitech.ac.jp

[1] Aichi Institute of Technology, 1247, Yachigusa, Yakusa-cho, Toyota, Aichi 470-0392, Japan

[2] Panasonic Smart Factory Solutions Co., Ltd., Osaka, Japan

[3] Japan Advanced Institute of Science and Technology, 1-1, Asahidai, Nomi, Ishikawa 923-1292, Japan

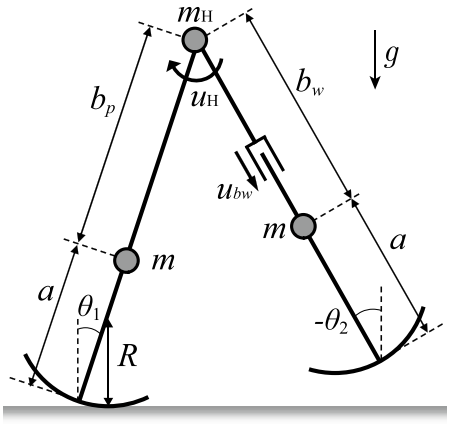

Fig. 1 Model of biped robot with telescopic swing leg

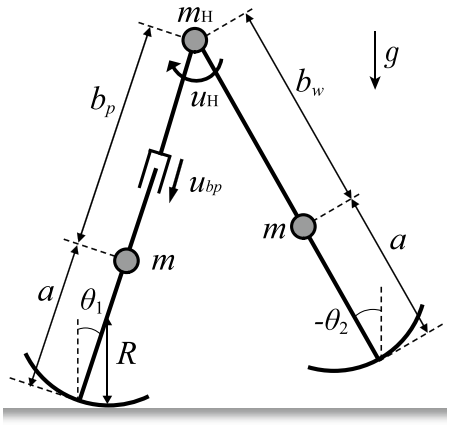

Fig. 2 Model of biped robot with telescopic support leg

numerical integral is partially used. Finally, we show the effect of swing-leg/support-leg telescopic motion on the stability.

2 Modeling and control

2.1 Model of robots

Figures 1 and 2 show biped robot models. The robots consist of two telescopic legs, support and swing legs, with concentrated mass m [kg] and the legs are connected on a hip joint. The legs have semicircular feet, whose radius is R [m]. A torso is replaced by a concentrated mass m_{H} [kg] on the hip joint (total mass $M := 2m + m_{\mathrm{H}}$ [kg]). The distance between the leg's mass and the edge of the leg is a [m]. The robots have actuators on the hip joints and their legs, and their input torque and forces are u_{H} [Nm] and u_{bi} [N] ($i = p, w$), respectively. The actuator on the hip joint swings the swing leg and the actuators on the legs control their leg length b_i [m] ($i = p, w$), where b_p and b_w are the lengths from the hip joints to support-leg and swing-leg masses, respectively. When the swing or support leg is pumped, the support or swing leg is locked for their length to be constant, b [m]. Angular positions of the support and swing legs from the vertical axis are designated by θ_1 [rad] and θ_2 [rad], respectively.

Dynamics of the robot consists of the equation of motion during the stance phase and impact equation at heel strike. Since it has already shown that the heel strike always becomes stable in [9], in this paper, we focus on stability of the stance phase in biped robots with telescopic legs.

The equation of motion of the robots is given by

$$\boldsymbol{M}(\boldsymbol{x})\ddot{\boldsymbol{x}} + \boldsymbol{h}(\boldsymbol{x}, \dot{\boldsymbol{x}}) = \begin{bmatrix} 1 & 0 \\ -1 & 0 \\ 0 & 1 \end{bmatrix} \begin{bmatrix} u_{\mathrm{H}} \\ u_{bi} \end{bmatrix} := \boldsymbol{S}\boldsymbol{u}, \tag{1}$$

where $\boldsymbol{x} = \begin{bmatrix} \theta_1 & \theta_2 & b_i \end{bmatrix}^{\mathrm{T}}$ is a generalized coordinate vector.

Next, we explain impact equation. A completely inelastic collision is assumed to occur at heel strike and the hip joint and telescopic-leg length are mechanically locked at heel strike, that is $\theta_H := \theta_1 - \theta_2 = 2\alpha$ [rad] and $b_i = b$ [m]. Then, angular velocities of the swing and support legs are identical, that is, $\dot{\theta}_1^- = \dot{\theta}_2^- := \dot{\theta}^-, \dot{\theta}_1^+ = \dot{\theta}_2^+ := \dot{\theta}^+$, where superscripts "−" and "+" represent states immediately before and after heel strike, respectively. In these assumptions, impact equation is given by

$$\dot{\boldsymbol{x}}^+ = \boldsymbol{H}\dot{\boldsymbol{x}}^-. \tag{2}$$

2.2 Linearized system and its control

The bookkeeping parameter ϵ is introduced, and the unknown variables are assumed as

$$\theta_j, \dot{\theta}_j, \ddot{\theta}_j, \dot{b}_i, \ddot{b}_i \in O(\epsilon) \quad (j = 1, 2). \tag{3}$$

Expanding $\sin\theta_j$ and $\cos\theta_j$ in Eq. (1) into Maclaurin series, we can obtain Eq. (1) under the order assumption Eq. (3) within the accuracy of $O(\epsilon)$ as

$$\boldsymbol{M}_0(b_i)\ddot{\boldsymbol{x}} + \boldsymbol{h}_0(\boldsymbol{x}, \dot{\boldsymbol{x}}) = \boldsymbol{S}\boldsymbol{u}. \tag{4}$$

Let leg length b_i and hip joint angle θ_{H} be control outputs. Then, output vector is given by

$$\boldsymbol{y} = \boldsymbol{S}^{\mathrm{T}}\boldsymbol{x} = \begin{bmatrix} \theta_{\mathrm{H}} & b_i \end{bmatrix}^{\mathrm{T}}. \tag{5}$$

The second-order derivative of $\boldsymbol{y}$ with respect to time becomes

$$\ddot{\boldsymbol{y}} = \boldsymbol{S}^{\mathrm{T}}\ddot{\boldsymbol{x}} = \boldsymbol{S}^{\mathrm{T}}\boldsymbol{M}_0^{-1}\left(\boldsymbol{S}\boldsymbol{u} - \boldsymbol{h}_0\right). \tag{6}$$

We assume that postures of the robots at heel strike are constant. Then, the controller to track desired trajectories $\boldsymbol{y}_{\mathrm{d}}(t) := \begin{bmatrix} \theta_{\mathrm{Hd}}(t) & b_{i\mathrm{d}}(t) \end{bmatrix}^{\mathrm{T}}$ strictly are given by

$$\boldsymbol{u} = \left(\boldsymbol{S}^{\mathrm{T}}\boldsymbol{M}_0^{-1}\boldsymbol{S}\right)^{-1}\left(\ddot{\boldsymbol{y}}_{\mathrm{d}}(t) + \boldsymbol{S}^{\mathrm{T}}\boldsymbol{M}_0^{-1}\boldsymbol{h}_{0\cdot}\right) \tag{7}$$

Substituting Eq. (7) into Eq. (4) and multiplying the resulting equation by $\boldsymbol{M}_0^{-1}$ from the left side, we can obtain

$$\begin{aligned}\ddot{\boldsymbol{x}} + \boldsymbol{M}_0^{-1}\left(\boldsymbol{I} - \boldsymbol{S}\left(\boldsymbol{S}^{\mathrm{T}}\boldsymbol{M}_0^{-1}\boldsymbol{S}\right)^{-1}\boldsymbol{S}^{\mathrm{T}}\boldsymbol{M}_0^{-1}\right)\boldsymbol{h}_0 \\ = \boldsymbol{M}_0^{-1}\boldsymbol{S}\left(\boldsymbol{S}^{\mathrm{T}}\boldsymbol{M}_0^{-1}\boldsymbol{S}\right)^{-1}\ddot{\boldsymbol{y}}_{\mathrm{d}}(t).\end{aligned} \tag{8}$$

The third row of Eq. (8) is rearranged as

$$\ddot{b}_1 = \ddot{b}_{1\mathrm{d}}(t). \tag{9}$$

If $b_i = b_{i\mathrm{d}}(0)$ and $\dot{b}_i = \dot{b}_{i\mathrm{d}}(0)$ are satisfied immediately after heel strike, the input (7) achieves $b_i = b_{i\mathrm{d}}(t)$. Note that time t is reset at every heel strike.

Subtracting the second row from the first row in Eq. (8), we can obtain

$$\ddot{\theta}_1 - \ddot{\theta}_2 = \ddot{\theta}_{\mathrm{Hd}}(t). \tag{10}$$

In the same way as the leg length, the input (7) achieves $\theta_{\mathrm{H}} = \theta_{\mathrm{Hd}}(t)$.

2.3 Desired trajectories

2.3.1 Trajectory for leg length

The desired trajectory for the leg length, b_i, is given by

$$b_{i\mathrm{d}}(t_1) = \begin{cases} b \mp b_l \sum_{n=0}^{8} c_n t_1^n & (0 \le t_1 \le T_{\mathrm{set}1}), \\ b & (T_{\mathrm{set}1} < t_1), \end{cases} \tag{11}$$

where b_l [m] is telescopic distance, $t_1 = t - t_{d1}$ [s], t_{d1} [s] is the starting time of telescopic motion, and $T_{\mathrm{set}\,1}$ [s] is the settling time of the motion. Minus-plus sign of b_l correspond to the swing-leg/support-leg telescopic motion. Coefficients $c_n (n = 0, 1, \ldots, 8)$ are determined so that $b_{i\mathrm{d}}$ and the time derivatives satisfy the following initial, middle, and terminal conditions:

$$\begin{array}{ll} b_{i\mathrm{d}}(0) = b, & \dot{b}_{i\mathrm{d}}(0),\ \ddot{b}_{i\mathrm{d}}(0) = 0, \\ b_{i\mathrm{d}}(T_{\mathrm{set}1}/2) = b \mp b_l, & \dot{b}_{i\mathrm{d}}(T_{\mathrm{set}\,1}/2),\ \ddot{b}_{i\mathrm{d}}(T_{\mathrm{set}1}/2) = 0, \\ b_{i\mathrm{d}}(T_{\mathrm{set}1}) = b, & \dot{b}_{i\mathrm{d}}(T_{\mathrm{set}1}),\ \ddot{b}_{i\mathrm{d}}(T_{\mathrm{set}1}) = 0. \end{array} \tag{12}$$

2.3.2 Trajectory for hip angle

The desired trajectory for the hip joint angle, θ_{H}, is given by

$$\theta_{\mathrm{H\,d}}(t_2) = \begin{cases} -2\alpha + \sum_{n=0}^{5} d_n t_2^n & (0 \le t_2 \le T_{\mathrm{set}\,2}) \\ 2\alpha & (T_{\mathrm{set}\,2} < t_2), \end{cases} \tag{13}$$

where $t_2 = t - t_{d2}$ [s], t_{d2} [s] is the starting time of swinging a leg, $T_{\mathrm{set}\,2}$ [s] is the settling time of swing-leg motion, and 2α [rad] is the hip angle at heel strike. Coefficients $d_n (n = 0, 1, ..., 5)$ are determined so that θ_{Hd} and the time derivatives satisfy the following initial and terminal conditions:

$$\begin{array}{lll} \theta_{\mathrm{Hd}}(0) = -2\alpha, & \dot{\theta}_{\mathrm{Hd}}(0) = 0, & \ddot{\theta}_{\mathrm{Hd}}(0) = 0, \\ \theta_{\mathrm{Hd}}(T_{\mathrm{set}2}) = 2\alpha, & \dot{\theta}_{\mathrm{Hd}}(T_{\mathrm{set}2}) = 0, & \ddot{\theta}_{\mathrm{Hd}}(T_{\mathrm{set}2}) = 0. \end{array} \tag{14}$$

2.4 Linear time-varying system

The state vector $\boldsymbol{X} = \left[\ \theta_1\ \ \theta_2\ \ \dot{\theta}_1\ \ \dot{\theta}_2\ \right]^{\mathrm{T}}$ is introduced, and it is assumed that b_l is much less than b. Substituting input (7) into Eq. (4), the first and second rows of the resulting equation can be rearranged as

$$\dot{\boldsymbol{X}} = \boldsymbol{A}(t)\boldsymbol{X} + \boldsymbol{B}(t)\ddot{\theta}_{\mathrm{Hd}}(t), \tag{15}$$

where the above equation is linearly approximated for b_l. Note that the third rows of the resulting equation is $\ddot{b}_i = \ddot{b}_{i\mathrm{d}}(t)$. The system represented by Eq. (15) is time-varying. The matrix $\boldsymbol{A}(t) \in \mathbb{R}^{4\times4}$ is given by

$$\boldsymbol{A}(t) = \begin{cases} \boldsymbol{A}_1(t) & (0 \le t_1 \le T_{\mathrm{set}1}), \\ \boldsymbol{A}_2 & (\text{Otherwise}), \end{cases} \tag{16}$$

where $\boldsymbol{A}_2$ is constant.

3 Error transition equation

In this section, error transition equation similar to reference [9] is derived to evaluate the stability during the stance phase.

3.1 Transition matrix

The system represented by Eq. (15) is time-varying and its solution can be obtained as

$$\boldsymbol{X}(t) = \boldsymbol{\Phi}(t, t_0)\boldsymbol{X}_0 + \int_{t_0}^{t} \boldsymbol{\Phi}(t, \tau)\boldsymbol{B}(\tau)\ddot{\theta}_{\mathrm{Hd}}(\tau)\mathrm{d}\tau, \tag{17}$$

where $\boldsymbol{\Phi}(t, \tau) \in \mathbb{R}^{4\times4}$ is transition matrix given by

$$\begin{aligned}\boldsymbol{\Phi}(t, t_0) = \boldsymbol{I}_4 + \int_{t_0}^{t} \boldsymbol{A}(\sigma_1)\mathrm{d}\sigma_1 \\ + \int_{t_0}^{t} \boldsymbol{A}(\sigma_1) \int_{t_0}^{\sigma_1} \boldsymbol{A}(\sigma_2)\mathrm{d}\sigma_2\mathrm{d}\sigma_1 + \cdots.\end{aligned} \tag{18}$$

Note that when $\boldsymbol{A}(t) = \boldsymbol{A}_2$, the transition matrix is given by

$$\boldsymbol{\Phi}_2(t, T_{\mathrm{set}1}) = e^{\boldsymbol{A}_2(t - T_{\mathrm{set}1})}. \tag{19}$$

3.2 Derivation of error transition equation

The solutions of the system represented by Eq. (15) are difference depending on the values of t_{d1}, t_{d2}, $T_{\mathrm{set}\,1} + t_{d1}$ and

$T_{\text{set}\,2} + t_{d2}$. However, error transition equations in all the cases have the same form, which can be derived by subtracting steady state immediately before heel strike from that at the $k+1$th step as follows:

$$\begin{aligned}\Delta \boldsymbol{X}_{k+1}^{-} &= e^{\boldsymbol{A}_2(T^*-T_e)}\boldsymbol{\Phi}(T_e, t_{d1})e^{\boldsymbol{A}_2 t_{d1}}\Delta \boldsymbol{X}_k^{+} \\ &\quad + \boldsymbol{A}_2 \boldsymbol{X}_{\text{eq}}^{-}\Delta T_{k+1},\end{aligned} \tag{20}$$

where $T_e = T_{\text{set}\,1} + t_{d1}$. State at the kth step $\boldsymbol{X}_k$ and the period T_k are defined as $\boldsymbol{X}_k = \boldsymbol{X}_{\text{eq}} + \Delta \boldsymbol{X}_k$ and $T_k = T^* + \Delta T_k$, where T^* and $\boldsymbol{X}_{\text{eq}}$ are step period and state of steady walking, respectively. Equation (20) is linearly approximated for ΔT_k and $\Delta \boldsymbol{X}$.

From the assumption that the posture at heel strike is constant, multiplying $\boldsymbol{p} = \begin{bmatrix} 1 & 1 & 0 & 0 \end{bmatrix}$ from left side, we can obtain

$$\begin{aligned}\boldsymbol{p}\Delta \boldsymbol{X}_{k+1}^{-} &= \Delta\theta_1 + \Delta\theta_2 = 0 \\ &= \boldsymbol{p}e^{\boldsymbol{A}_2(T^*-T_e)}\boldsymbol{\Phi}(T_e, t_{d1})e^{\boldsymbol{A}_2 t_{d1}}\Delta \boldsymbol{X}_k^{+} \\ &\quad + \boldsymbol{p}\boldsymbol{A}_2 \boldsymbol{X}_{\text{eq}}^{-}\Delta T_{k+1},\end{aligned} \tag{21}$$

and then

$$\Delta T_{k+1} = -\frac{\boldsymbol{p}e^{\boldsymbol{A}_2(T^*-T_e)}\boldsymbol{\Phi}(T_e, t_{d1})e^{\boldsymbol{A}_2 t_{d1}}}{\boldsymbol{p}\boldsymbol{A}_2 \boldsymbol{X}_{\text{eq}}^{-}}\Delta \boldsymbol{X}_k^{+}. \tag{22}$$

Note that the vector $\boldsymbol{p}$ is not uniquely determined. Substituting ΔT_{k+1} into Eq. (20), we can obtain

$$\begin{aligned}\Delta \boldsymbol{X}_{k+1}^{-} &= \left(\boldsymbol{I}_4 - \frac{\boldsymbol{A}_2 \boldsymbol{X}_{\text{eq}}^{-}\boldsymbol{p}}{\boldsymbol{p}\boldsymbol{A}_2 \boldsymbol{X}_{\text{eq}}^{-}}\right)e^{\boldsymbol{A}_2(T^*-T_e)} \\ &\quad \times \boldsymbol{\Phi}(T_e, t_{d1})e^{\boldsymbol{A}_2 t_{d1}}\Delta \boldsymbol{X}_k^{+} \\ &:= \boldsymbol{Q}\Delta \boldsymbol{X}_k^{+},\end{aligned} \tag{23}$$

It is assumed that the posture is constant and the hip joint angular velocity equals to zero at heel strike, and hence

$$\Delta \boldsymbol{X}^{\pm} = \begin{bmatrix} \Delta\theta_1 & \Delta\theta_2 & \Delta\dot{\theta}_1^{\pm} & \Delta\dot{\theta}_2^{\pm} \end{bmatrix}^{\text{T}} = \begin{bmatrix} 0 & 0 & \Delta\dot{\theta}_1^{\pm} & \Delta\dot{\theta}_i^{\pm} \end{bmatrix}^{\text{T}}.$$

Therefore, the state error vector $\Delta \boldsymbol{X}_k^{\pm}$ has following form:

$$\Delta \boldsymbol{X}_k^{\pm} = 2\boldsymbol{v}\Delta\dot{\theta}_k^{\pm}, \quad \boldsymbol{v} := \begin{bmatrix} 0 & 0 & 1/2 & 1/2 \end{bmatrix}^{\text{T}} \tag{24}$$

and the relation

$$\Delta\dot{\theta}_k^{\pm} = \boldsymbol{v}^{\text{T}}\Delta \boldsymbol{X}_k^{\pm} \tag{25}$$

holds. Then, Eq. (23) can be rewritten as

$$\Delta\dot{\theta}_{(k+1)}^{-} = \bar{Q}\Delta\dot{\theta}_k^{+}, \quad \bar{Q} := 2\boldsymbol{v}^{\text{T}}\boldsymbol{Q}\boldsymbol{v}. \tag{26}$$

The value of $\bar{Q}$ represents error convergence property during the stance phase. If the value of $|\bar{Q}|$ is less than one, the stance phase is stable in the sense that error from steady walking decreases during the stance phase. In addition, if the value of $|\bar{Q}|$ is smaller, the walking state converges to the steady one more quickly.

Our approach needs to numerically calculate step period and steady state immediately before heel strike. The method using Poincáre map also needs numerical calculation and eigenvalues determined by Poincáre map depend on the values of perturbation. Our approach, however, has the advantage that the scalar transition function for the state error can be uniquely determined.

Table 1 Physical parameters of biped robots

$a = b$	0.5	m	R	0.3	m
m	5.0	kg	m_{H}	10.0	kg

4 Numerical results

We evaluated the gait efficiency in terms of the stability of hybrid zero dynamics (the convergence speed, $\bar{Q}$) and walking speed. Note that, we calculate and show the stability ($\bar{Q}$) and the walking period only in the case that the stable walking is generated.

4.1 Approximation of transition matrix

The transition matrix Eq. (18) is approximately determined as follows:

$$\boldsymbol{\Phi}(T_{\text{set}}, 0) = \boldsymbol{I}_4 + \sum_{i=1}^{N}\boldsymbol{\Phi}_i(T_{\text{set}}, 0), \tag{27}$$

where

$$\boldsymbol{\Phi}_i(t, t_0) = \int_{t_0}^{t} \text{d}t_1 \cdots \int_{t_0}^{t_{i-1}} \text{d}t_i \boldsymbol{A}_1(t_1)\cdots\boldsymbol{A}_1(t_i). \tag{28}$$

In numerical simulations, we set N to 16, because $\boldsymbol{\Phi}_i(T_e, t_{d1})$ is almost converging to a constant value more than $N = 16$.

4.2 Typical walking

Figures 3 and 4 are the stick diagrams of steady walking with swing-leg and support-leg telescopic motion. The values of the parameters of the robots and desired trajectory are listed in Tables 1 and 2, and the hip joint angle at heel strike is set to $2\alpha = \pi/10$ [rad].

It can be seen that introducing the starting time of the telescopic motion of the swing and support legs is contracted and expanded in the latter half. The generated walking

Table 2 Parameters of desired trajectory

$\|b_l\|$	0.1	m	2α	$\pi/10$	rad
$T_{\text{set 1}}$	0.2	s	t_{d1}	0.3	s
$T_{\text{set 2}}$	0.5	s	t_{d2}	0.0	s

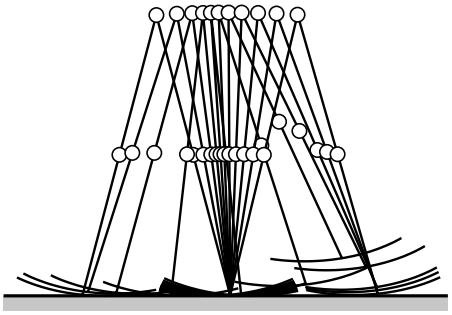

Fig. 3 Stick diagrams of typical walking via swing-leg telescopic motion

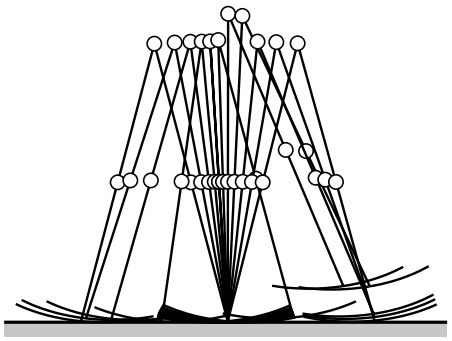

Fig. 4 Stick diagrams of typical walking via support-leg telescopic motion

motion has small step length, and hence, the effect of nonlinearity is comparatively small if the influences of the telescopic motion on the nonlinearity are also small.

4.3 Effect of swing-leg telescopic motion

Figure 5 plots $\bar{Q}$ and the walking period T_{eq} for three values of α with respect to b_l for swing-leg telescopic motion. The values of the desired trajectory are listed in Table 2 except for b_l and α. The hip joint angles at heel strike are set to $2\alpha = \pi/12, \pi/11$, and $\pi/10$ [rad], which are represented by triangle, cross, and circle, respectively. It can be seen that $\bar{Q}$ monotonically decreases and the step period increases as b_l increases. The hip joint angles at heel strike are constant, and the walking speed is inversely proportional to the step period. Therefore, the walking speed decreases as the step period increases.

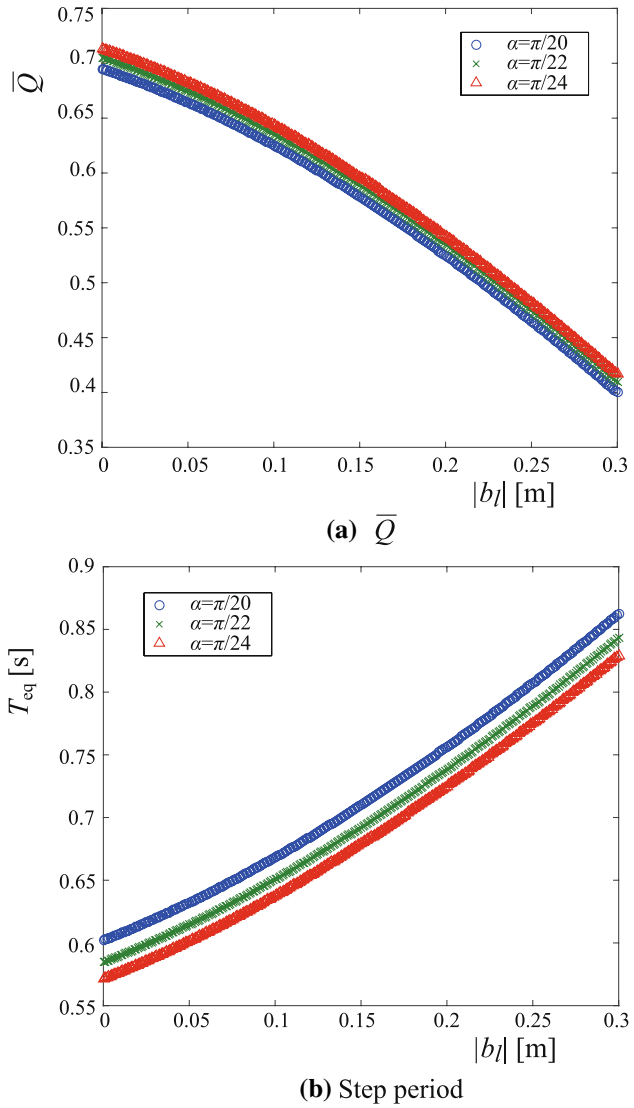

Fig. 5 Effect of b_l on $\bar{Q}$ and step period in swing-leg telescopic motion

In [9, 10], it was shown that the deadbeat modes, where the state error is settled to zero through a single step, tends to appear in the case that the robot marginally overcomes the potential barrier. If the kinetic energy after heel strike is sufficiently large, that is, the walking speed of the robot is large, the robot easily overcomes the potential barrier. These results mean that slower walking is more stable, and are consistent with the above results.

The effect of the telescopic motion on the mechanical energy of the robot is given by

$$E_d = \int_{t_{d1}}^{T_{set1}} u_{bi}\dot{b}_i \mathrm{d}t. \tag{29}$$

We expected that the telescopic motions increase the mechanical energy of the robots like parametric excitation walking [4], that is $E_d > 0$. If $E_d > 0$, as the telescopic distance b_l increases the walking speed of the robot may increases, that is, the step period decreases. However, the step period increases as b_l increases. It is considered that the motions decrease mechanical energy in this paper. Therefore, the walking approaches to that the robot marginally overcomes the potential barrier as b_l increases.

Figure 6 plots $\bar{Q}$ and the walking period T_{eq}, for three values of α with respect to $T_{\text{set 1}}$. Here, $T_{\text{set 1}} + t_{d1} = 0.5$ [s]. It can be seen that $\bar{Q}$ decreases until optimal value of T_{set1} and then increases. At the optimal values of T_{set1}, the step period is near maximum value. Similar to Fig. 5, slower walking is more stable.

Figure 7 plots $\bar{Q}$ and the walking period T_{eq}, for three values of α with respect to R. It can be seen that $\bar{Q}$ and the step period monotonically decrease as R increases. In this case, faster walking is more stable, and this result is inconsistent with above results. This is because semicircular feet stabilize bipedal locomotion. Especially, when the foot radius increases, the support leg may avoid falling down like a tumbler toy. The foot effects are greater than disturbance rejection during the stance phase, and hence, $\bar{Q}$ decreases as R increases.

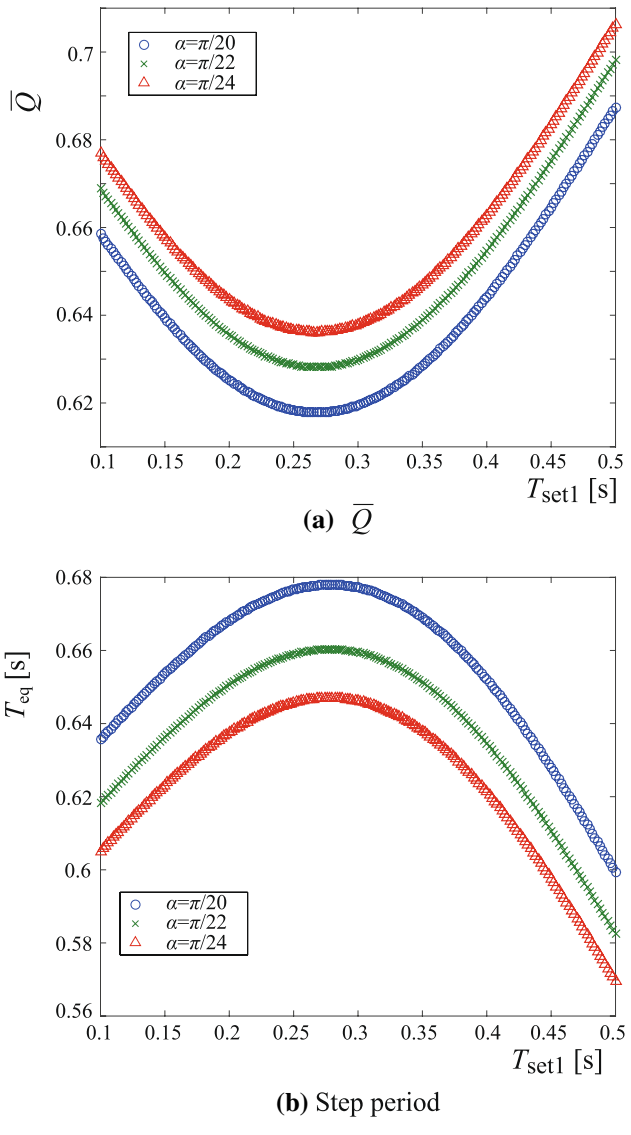

Fig. 6 Effect of $T_{\text{set 1}}$ on $\bar{Q}$ and step period in swing-leg telescopic motion

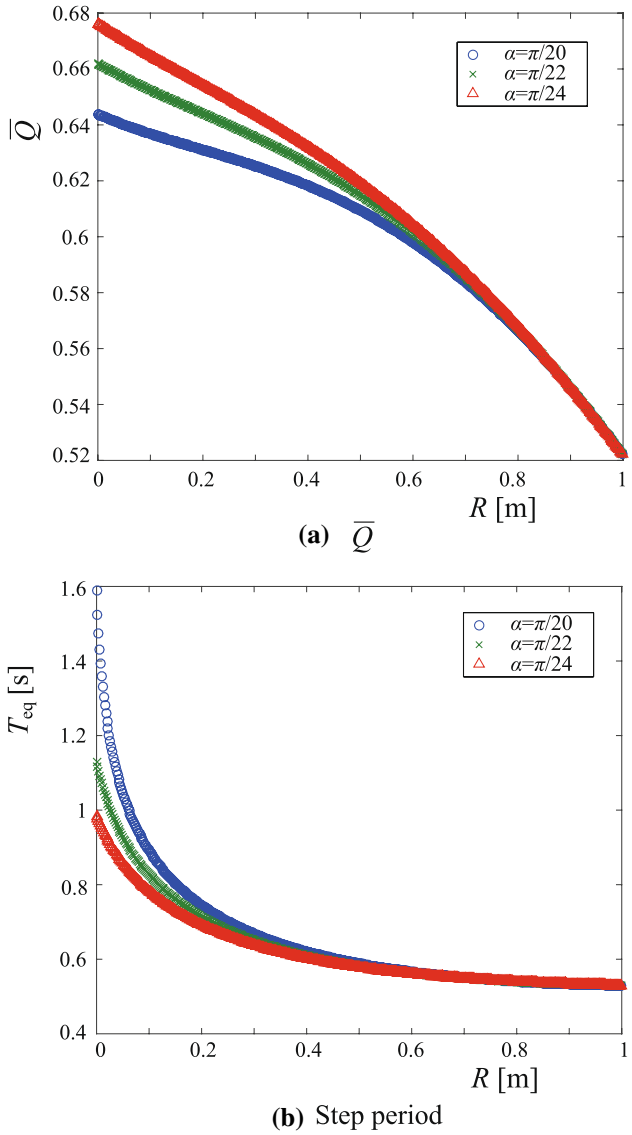

Fig. 7 Effect of R on $\bar{Q}$ and step period in swing-leg telescopic motion

4.4 Effect of support-leg telescopic motion

Figure 8 plots $\bar{Q}$ and walking period T_{eq} for three values of α with respect to b_l for support-leg telescopic motion. The values of the desired trajectory are listed in Table 2 except for b_l and α. It can be seen that $\bar{Q}$ monotonically decreases and the step period increases as b_l increases. These results are similar to those in the swing-leg telescopic motion, although the influences of the support-leg motion are less than those of the swing-leg motion.

Figure 9 plots $\bar{Q}$ and walking period T_{eq}, for three values of α with respect to $T_{set\,1}$. Here, $\bar{Q}$ decreases until optimal value of T_{set1} and then increases. At the optimal values of T_{set1}, the step period is near maximum value.

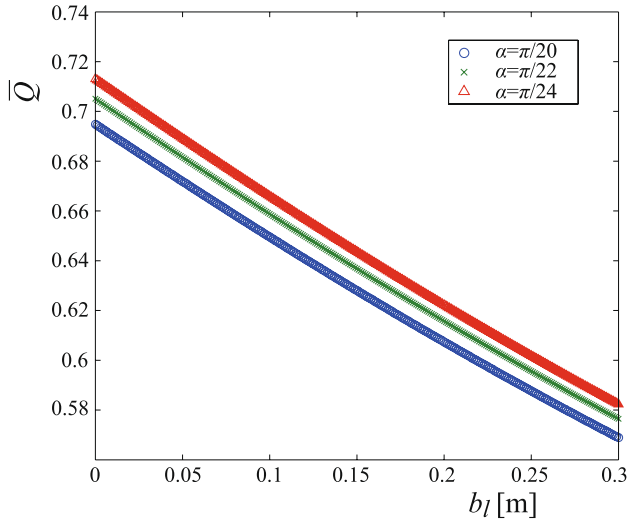

(a) $\bar{Q}$

(b) Step period

Fig. 8 Effect of b_l on $\bar{Q}$ and step period in support-leg telescopic motion

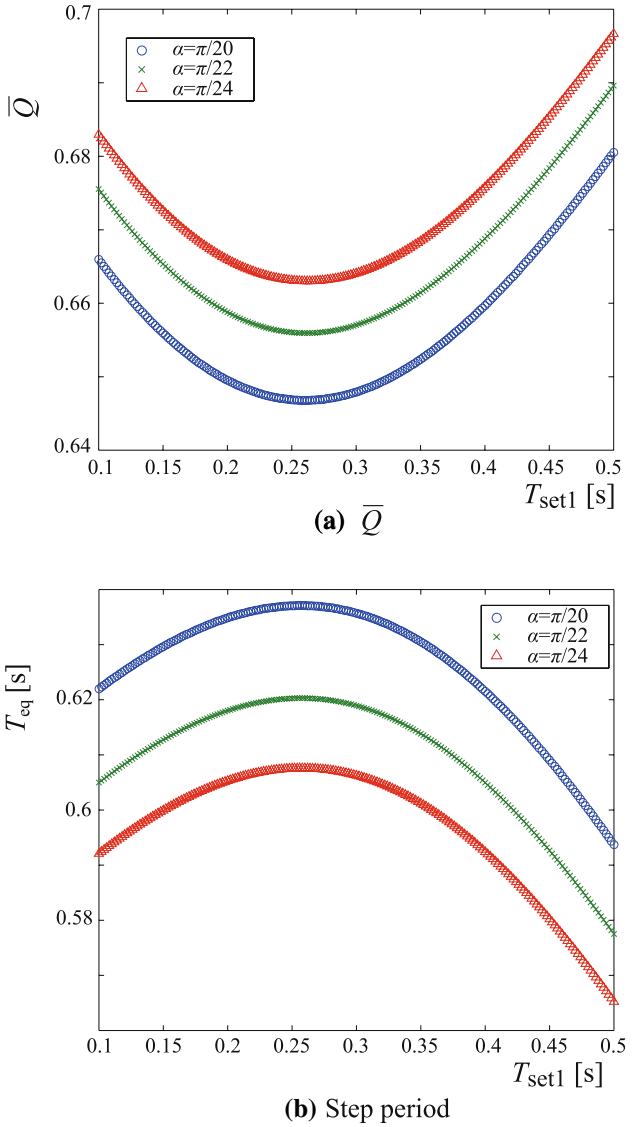

(a) $\bar{Q}$

(b) Step period

Fig. 9 Effect of $T_{set\,1}$ on $\bar{Q}$ and step period in support-leg telescopic motion

The results in Figs. 8 and 9 are similar to those in Figs. 5 and 6. The influences of the desired trajectories of the support-leg motion on the stability are less than that of the swing-leg motion.

Figure 10 plots $\bar{Q}$ and walking period T_{eq}, for three values of α with respect to R. It can be seen that $\bar{Q}$ decreases and turns to increase as R increases, while the step period monotonically decreases as R increases. Therefore, $\bar{Q}$ has the optimal value. Due to the telescopic motion of the support leg, COM of the support leg comes from and goes inside of the center of the semicircular foot, and the stability of the support leg like a tumbler toy is fluctuated. In addition, in the case of the support-leg telescopic motion, the robot kicks the ground by pumping the support legs, and hence, the effect of the semicircular foot is more complicated than

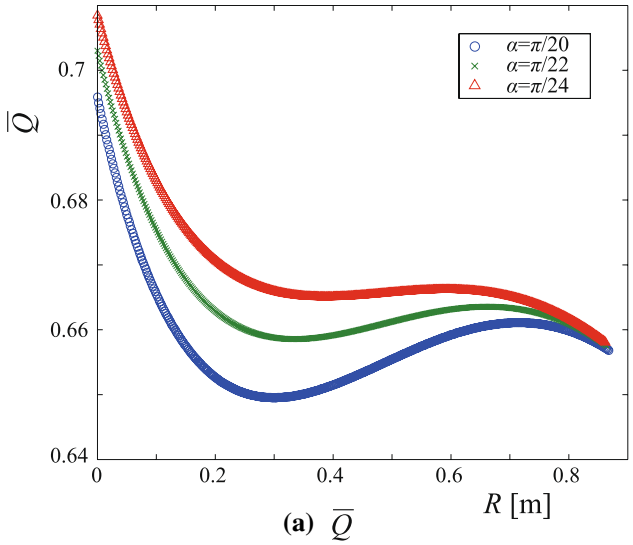

(a) $\bar{Q}$

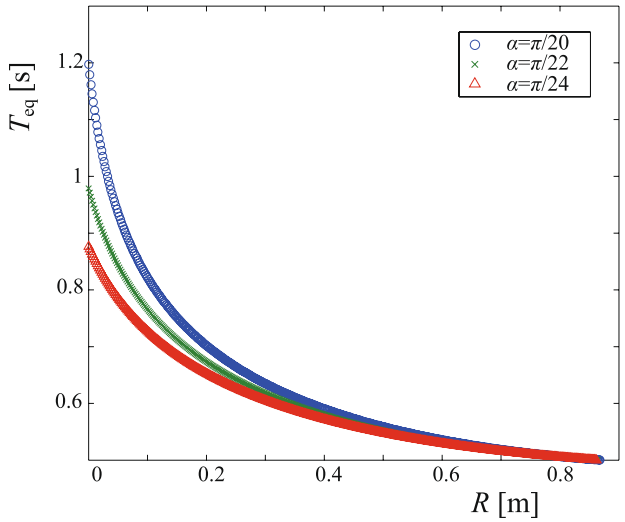

(b) Step period

Fig. 10 Effect of R on $\bar{Q}$ and step period in support-leg telescopic motion

in the case of the swing-leg telescopic motion. In addition, the range of the foot radius of the biped with the swing-leg telescopic motion is wider than that with the support-leg telescopic motion. This means that the biped with the swing-leg telescopic motion can walk for wider range of the foot radius in these parameters.

5 Conclusion

Stability of the biped robots with telescopic legs was investigated. The linearized equations of the robots were derived, and the error transition equations during the stance phase were uniquely determined. The results can be summarized as follows:

- Slower walking are more stable, because the error from steady walking gradually decreases during the stance phase.
- Walking using the swing-leg motion is more stable than that using the support-leg motion.
- The influences of the desired trajectories of the swing-leg motion on the stability is larger than that of the support-leg motion.

When b_l is large the linear approximation Eq. (15) is inaccurate. In the future, we need to compare the difference between the linearized model and nonlinear model using numerical integration to verify the validity of the linear approximation. In addition, numerical calculations are needed to determine the stability of steady walks. In the future, high accurate and analytical method to determine the stability will be developed.

Acknowledgements This research was partially supported by Grabt-in-Aid for Scientific Research (C) no. 16K06154, provided by the Japan Society for the Promotion of Science (JSPS).

References

1. McGeer T (1990) Passive dynamic walking. Int J Robot Res 9(2):62–82
2. Goswami A, Thuilot B, Espiau B (1996) Compass-like biped robot Part I: Stability and bifurcation of passive gaits. IINRIA Res Rep 2996
3. Garcia M, Chatterjee A, Ruina A, Coleman M (1998) The simplest walking model: stability, complexity, and scaling. J Biomech Eng 120:281–288
4. Asano F, Luo ZW (2008) Energy-efficient and high-speed dynamic biped locomotion based on principle of parametric excitation. IEEE Trans Robot 24(6):1289–1301
5. Hanazawa Y, Asano F (2015) High-speed biped walking using swinging-arms based on principle of up-and-down wobbling mass. In: Proc. the 2015 IEEE international conference on robotics and automation, pp 5191–5196
6. Schwab AL, Wisse M (2001) Basin of attraction of the simplest walking model. ASME 2001 design engineering technical conferences, pp 1–9
7. Hobbelen DGE, Wisse M (2007) A disturbance rejection measure for limit cycle walkers: the gait sensitivity norm. IEEE Trans Robot 23:1213–1224
8. Hirata K, Kokame H (2003) Stability analysis of linear systems with state jump-motivated by periodic motion control of passive walker. In: Proc. of IEEE conference on control applications, pp 949–953
9. Asano F (2015) Stability analysis of underactuated compass gait based on linearization of motion. Multibody Syst Dyn 33(1):93–111
10. Asano F (2015) Fully analytical solution to discrete behavior of hybrid zero dynamics in limit cycle walking with constraint on impact posture. Multibody Syst Dyn 35(2):191–213